J|A|C|S
ARTICLES
Published on Web 04/20/2002

Dissociation Kinetics of Energy-Selected Cp_2Mn^+ Ions Studied by Threshold Photoelectron-Photoion Coincidence Spectroscopy

Yue Li, Bálint Sztáray, and Tomas Baer*

Contribution from the Department of Chemistry, University of North Carolina, Chapel Hill, North Carolina 27599-3290

Received December 10, 2001

Abstract: Threshold photoelectron-photoion coincidence spectroscopy has been used to investigate the dissociation kinetics of the manganocene ion, Cp_2Mn^+ ($Cp = \eta^5$-cyclopentadienyl). The Cp loss reaction was found to be extremely slow over a large ion internal energy range. By simulating the measured asymmetric time-of-flight peak shapes and breakdown diagram, the 0 K thermochemical dissociation limit for $CpMn^+$ production was determined to be 9.55 ± 0.15 eV. A $CpMn^+-Cp$ bond energy of 3.43 eV was obtained by combining this $CpMn^+ + Cp$ dissociation limit with the Cp_2Mn adiabatic ionization energy of 6.12 ± 0.07 eV. Combining the measured onset with known heats of formation of Cp and Mn^+, the $Cp-Mn^+$ bond energy was determined to be 3.38 ± 0.15 eV. These results lead to 298 K heats of formation of Cp_2Mn^+ and $CpMn^+$ of 863 ± 7 and 935 ± 16 kJ/mol, respectively. Finally, by combining these results with a previous measurement of the $CpMn(CO)_3 \rightarrow CpMn^+ + 3CO + e^-$ dissociation limit, we arrive at a new value for $\Delta_f H^\circ_{298K}(CpMn(CO)_3)$ of -424 ± 17 kJ/mol.

Introduction

The physical and chemical properties of organometallic compounds are important for understanding the formation and cleavage of the chemical bonds between metals and ligands and the mechanisms of catalytic reactions.[1] However, for many organometallic compounds, especially for the fragment molecules and ions, the thermochemical data are poorly known because of the difficulty in determining heats of formation and dissociation onsets. Fragment ion appearance energies (AE) obtained by variable energy electron ionization have been reported. However, electron ionization results often have large errors because the energy resolution is poor, and the sample thermal energy and kinetic shift are generally ignored in the data analysis.

In a recent paper,[2] we reported the results of the dissociation kinetics of the $CpMn(CO)_3^+$ ion, an important organometallic compound, obtained using threshold photoelectron-photoion coincidence (TPEPICO) spectroscopy. Ions were energy-selected by this technique, and through simulation for the experimental data with the statistical theory of unimolecular reactions, the AE values of fragment ions were accurately determined, from which accurate bond energies could be obtained.

In this study we report on the TPEPICO results of the dissociation kinetics of a related organometallic compound, the manganocene ion (Cp_2Mn^+). Manganocene is of particular interest because in liquid or solid solutions, its magnetic properties are consistent with high-spin ($^6A_{1g}$) as well as low-spin ($^2E_{2g}$) ground states[3−5] while other metallocenes are low spin. The high-spin−low-spin equilibrium depends on the molecular environment and temperature. In the gas phase, the He(I) and He(II) photoelectron spectrum studies have shown that Cp_2Mn is predominantly a high-spin compound with a $(e_{2g})^2(a_{1g})^1(e_{1g})^2$ ground-state configuration.[6,7]

Several groups have measured the photoelectron spectra (PES) of Cp_2Mn.[6−8] However, their interpretation is far from trivial. Spin selection rules suggest that the dominant PES peak at 6.91 eV be assigned to the $^6A \rightarrow {}^5E$ transition.[9] However, because the most stable configuration in the ion is the ^3E state, the adiabatic IE is considerably lower, a claim supported by the very broad peak in the PES of Cp_2Mn. A small low-energy peak at 6.26 eV in the PES has been assigned to the vertical transition, $^2E \rightarrow {}^3E$, and because the ^2E and ^6A states in the neutral Cp_2Mn are nearly the same energy, this PES peak is felt to be close to the adiabatic IE. This is consistent with an adiabatic free energy of ionization of 6.18 ± 0.07 eV reported by Ryan et al.,[9,10] which was based on electron-transfer equilibrium studies

* Corresponding author. E-mail: baer@unc.edu.

(1) Martinho Simões, J. A.; Beauchamp, J. L. *Chem. Rev.* **1990**, *90*, 629−688.
(2) Li, Y.; Sztáray, B.; Baer, T. *J. Am. Chem. Soc.* **2001**, *123*, 9388−9396.
(3) Switzer, M. E.; Wang, R.; Rettig, M. F.; Maki, A. H. *J. Am. Chem. Soc.* **1974**, *96*, 7669−7674.
(4) Ammeter, J. H.; Bucher, R.; Oswald, N. *J. Am. Chem. Soc.* **1974**, *96*, 7833−7835.
(5) Cozak, D.; Gauvin, F.; Demers, J. *Can. J. Chem.* **1986**, *64*, 71−75.
(6) Evans, S.; Green, M. L. H.; Jewitt, B.; King, G. H.; Orchard, A. F. *J. Chem. Soc., Faraday Trans. 2* **1974**, *70*, 356−376.
(7) Cauletti, C.; Green, J. C.; Kelly, M. R.; Powell, P.; Tilborg, J. V.; Robbins, J.; Smart, J. *J. Electron Spectrosc. Relat. Phenom.* **1980**, *19*, 327−353.
(8) Rabalais, J. W.; Werme, L. O.; Bergmark, T.; Karlsson, L.; Hussain, M.; Siegbahn, K. *J. Chem. Phys.* **1972**, *57*, 1185−1192.
(9) Ryan, M. F.; Eyler, J. R.; Richardson, D. E. *J. Am. Chem. Soc.* **1992**, *114*, 8611−8619.
(10) Ryan, M. F.; Richardson, D. E.; Lichtenberger, D. L.; Gruhn, N. E. *Organometallics* **1994**, *13*, 1190−1199.

using Fourier transform ion cyclotron resonance mass spectrometry. Because spin selection rules are readily violated in chemical reactions, this transition most likely connects the ground-state neutral with the ground-state ion structures. A knowledge of the entropy of ionization would permit us to convert this to an ionization energy.

Two electron impact ionization studies of Cp_2Mn^+ ion dissociation energies have been reported. Early work of Müller and D'or[11] using electron ionization mass spectrometry reported appearance energies of $CpMn^+$ and Mn^+ of 11.09 and 13.6 eV, respectively. However, as indicated previously, these values are not very reliable because they neglected the kinetic shift of these onsets due to the slow reaction rate at the dissociation limit. A recent study by Opitz[12] has taken considerably more care to take into account the kinetic shift. In this study, the dissociation onsets were measured by monitoring the fragment ions generated from metastable parent ions, thereby detecting the onsets at a much lower energy corresponding to ions that dissociate in the tens of microsecond range. The reported onsets for $CpMn^+$ and Mn^+ were 9.36 and 12.57 eV, respectively.

Experimental Approach

The TPEPICO apparatus has been described in detail previously.[13] Briefly, room-temperature sample vapor was leaked into the experimental chamber through a 1.5 mm diameter inlet and then was ionized with vacuum ultraviolet (VUV) light from a hydrogen discharge lamp dispersed by a 1 m normal incidence monochromator. The VUV wavelengths were calibrated by using the hydrogen Lyman-α line. The ions and the electrons were extracted in opposite directions with an electric field of 20 V/cm. Threshold photoelectrons were selected by a steradiancy analyzer[14] that consists of a flight tube with small apertures that discriminate against energetic electrons. Further discrimination was provided by a hemispherical electrostatic sector analyzer, resulting in a 35 meV combined photon and electron energy resolution. The ions were accelerated to 100 eV in the first 5 cm long acceleration region and then were accelerated to 220 eV in a short second region. The ions were detected after drifting through a 30 cm field-free drift region. The electrons and ions were detected with a channeltron electron multiplier and a multichannel plate detector, respectively. The electron and ion signals served as start and stop pulses for measuring the ion time-of-flight (TOF), and the TOF for each coincidence event was stored on a multichannel pulse height analyzer. TOF distributions were obtained in 1 to 48 h depending on the photon intensity and the desired spectrum quality.

The TPEPICO spectra were used for two purposes. First, the fractional abundances of the precursor and the product ions were measured as a function of the photon energy (breakdown diagram). Second, the $CpMn^+$ product ion TOF distributions were measured at energies close to the dissociation limit for this Cp loss reaction. Slowly dissociating (metastable) ions decay in the first acceleration region. The resulting product ion TOF distributions, which are asymmetrically broadened toward long TOF, can be analyzed to extract the ion dissociation rates as a function of ion internal energy. These two types of information were used together in the data analysis.

The manganocene sample ($(C_5H_5)_2Mn$, 98%, Strem Chemicals) was used without further purification.

Quantum Chemical Calculations. Reliable vibrational frequencies and rotational constants of the equilibrium structures for relevant neutral and ionic species are required for the simulation of the experimental data. Thus, quantum chemical calculations were performed by using the Gaussian-98 package[15] on the Origin 2000 computers at UNC−Chapel Hill and NC Supercomputing Center. Briefly, the neutral or ionic Cp_2Mn, Cp_2Mn^+, $CpMn^+$, and C_5H_5 structures were optimized at the Hartree−Fock (HF) level of theory. The 6-31G(d) basis set was chosen for the carbon and hydrogen atoms and the LANL2DZ basis set[16,17] was chosen for the manganese atom. Stationary points were confirmed through the calculations of harmonic vibrational frequencies. As discussed in the Introduction, neutral Cp_2Mn in the ground state is a mixture of high-spin sextet and low-spin doublet states with the high-spin state being slightly lower in energy, and thus dominant, while the ground state of the Cp_2Mn^+ ion is a triplet (^3E).[9] Because of the two neutral contributing spin states, and because DFT calculations[18] at the BLYP/DNP level have not been successful in reproducing the experimental energy ordering in the neutral molecule, we analyzed the data with vibrational frequencies from both low-spin and high-spin states. For the low-spin case, the spin multiplicities of neutral and ionic Cp_2Mn were set to be 2 and 1, respectively, while for the high-spin state, the spin multiplicities were 6 and 3.

The geometry of the Cp_2M molecules (M = V, Co, Ni) in the crystal is staggered (the D_{5d} point group),[19−22] but ferrocene and the other 3d metallocenes in the gas phase are found to be eclipsed (D_{5h}).[7,23−25] Because DFT calculations[18] predicted that the eclipsed conformer is 4 kJ/mol more stable than the staggered conformer, we initially restrained the neutral and ionic Cp_2Mn to the D_{5d} or D_{5h} symmetry for both low-spin and high-spin states. However, our calculations showed that these structures have at least three imaginary frequencies. Thus, the above symmetry restraints were relaxed.

Although we calculated various spin states for both the neutral and ionic Cp_2Mn, the only two states of importance for this study are the ground states of the neutral (^6A) and the ion (^3E), the structures of which are shown in Figure 1. As found by others,[18,25] the neutral ^6A state has eclipsed cyclopentadienyl rings. On the other hand, the ^3E state of the ion shows these rings to be staggered. The other major change upon ionization is that one of the C_5H_5 rings has moved substantially closer (by 0.12 Å) to the metal atom, while the other ring has remained as in the neutral molecule. The neutral Cp_2Mn structure in the sextet state has an imaginary frequency of -7 cm^{-1}, an analysis of which showed that this corresponds to the internal rotation of the Cp ring. Rather than performing further geometry optimizations, we simply used the first frequency of the low-spin state (2 cm^{-1}) instead of this negative frequency in the analysis of the data. As discussed later, since the frequency is treated as a rotor in the dynamic calculations, its value is of no concern.

(11) Müller, J.; D'or, L. *J. Organomet. Chem.* **1967**, *10*, 313−322.
(12) Opitz, J. *Eur. J. Mass Spectrom.* **2001**, *7*, 55−62.
(13) Baer, T.; Booze, J. A.; Weitzel, K. M. Photoelectron photoion coincidence studies of ion dissociation dynamics. In *Vacuum ultraviolet photoionization and photodissociation of molecules and clusters*; Ng, C. Y., Ed.; World Scientific: Singapore, 1991; pp 259−298.
(14) Baer, T.; Peatman, W. B.; Schlag, E. W. *Chem. Phys. Lett.* **1969**, *4*, 243−247.
(15) Frisch, M. J.; Trucks, G. W.; Schlegel, H. B.; Scuseria, G. E.; Robb, M. A.; Cheeseman, J. R.; Zakrzewski, V. G.; Montgomery, J. A., Jr.; Stratmann, R. E.; Burant, J. C.; Dapprich, S.; Millam, J. M.; Daniels, A. D.; Kudin, K. N.; Strain, M. C.; Farkas, O.; Tomasi, J.; Barone, V.; Cossi, M.; Cammi, R.; Mennucci, B.; Pomelli, C.; Adamo, C.; Clifford, S.; Ochterski, J.; Petersson, G. A.; Ayala, P. Y.; Cui, Q.; Morokuma, K.; Malick, D. K.; Rabuck, A. D.; Raghavachari, K.; Foresman, J. B.; Cioslowski, J.; Ortiz, J. V.; Stefanov, B. B.; Liu, G.; Liashenko, A.; Piskorz, P.; Komaromi, I.; Gomperts, R.; Martin, R. L.; Fox, D. J.; Keith, T.; Al-Laham, M. A.; Peng, C. Y.; Nanayakkara, A.; Gonzalez, C.; Challacombe, M.; Gill, P. M. W.; Johnson, B. G.; Chen, W.; Wong, M. W.; Andres, J. L.; Head-Gordon, M.; Replogle, E. S.; Pople, J. A. *Gaussian 98*, Revision A.7; Gaussian, Inc.: Pittsburgh, PA, 1998.
(16) Wadt, W. R.; Hay, P. J. *J. Chem. Phys.* **1985**, *82*, 284−298.
(17) Dunning, T. H., Jr.; Hay, P. J. In *Modern Theoretical Chemistry*; Schaefer, H. F. I., Ed.; Plenum: New York, 1976; pp 1−28.
(18) Matsuzawa, N.; Seto, J.; Dixon, D. A. *J. Phys. Chem. A* **1997**, *101*, 9391−9398.
(19) Seiler, P.; Dunitz, J. D. *Acta Crystallogr., Sect. B* **1980**, *36*, 2255−2260.
(20) Bünder, W.; Weiss, E. *J. Organomet. Chem.* **1975**, *92*, 65−68.
(21) Antipin, M. Y.; Lobkovskii, E. B.; Semenenko, K. N.; Soloveichik, J. L.; Struchkov, Y. T. *J. Struct. Chem. (Engl. Transl.)* **1979**, *20*, 810−811.
(22) Ketkov, S. Y.; Domrachev, G. A. *Inorg. Chim. Acta* **1990**, *178*, 233−242.
(23) Almenningen, A.; Gard, E.; Haaland, A.; Brunvoll, J. *J. Organomet. Chem.* **1975**, *88*, 181−189.
(24) Haaland, A.; Lusztyk, J.; Brunvoll, J.; Starowieyski, K. B. *J. Organomet. Chem.* **1975**, *85*, 279−285.
(25) Mayor-López, M. J.; Weber, J. *Chem. Phys. Lett.* **1997**, *281*, 226−232.

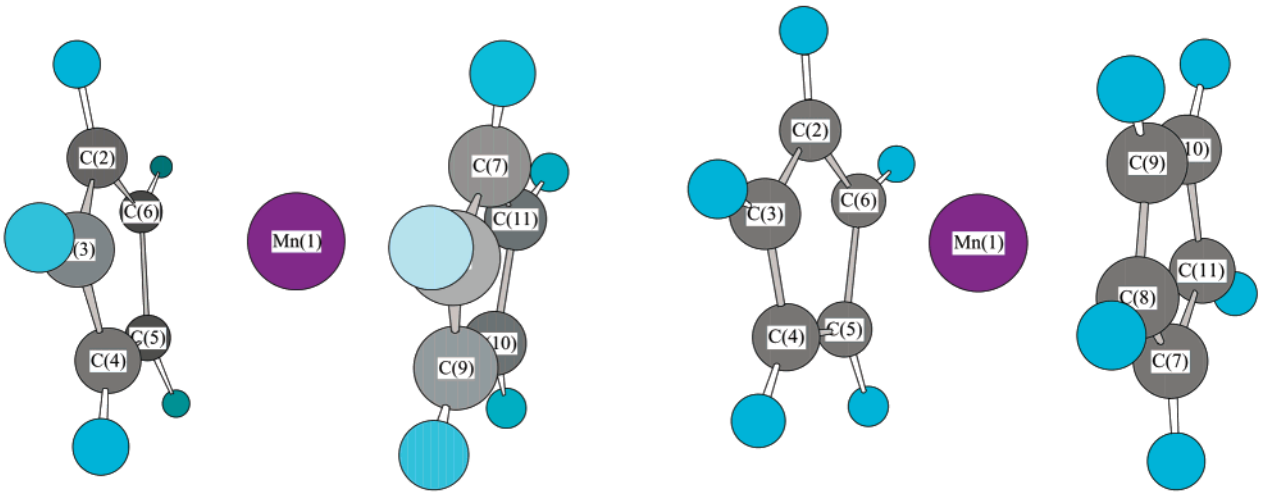

Cp_2Mn (6)
C_2-Mn=2.469 C_4-Mn=2.490 C_6-Mn=2.478
C_7-Mn=2.468 C_9-Mn=2.491 C_{11}-Mn=2.478

Cp_2Mn^+ (3)
C_2-Mn=2.325 C_4-Mn=2.309 C_6-Mn=2.340
C_7-Mn=2.491 C_9-Mn=2.446 C_{11}-Mn=2.451

Figure 1. Calculated equilibrium structures and main geometrical parameters of Cp_2Mn and Cp_2Mn^+ obtained at the HF/6-31G*: LANL2DZ level. The numbers in parentheses are the spin multiplicities.

Table 1. Frequencies (in cm^{-1}) Used for the Energy Distribution and RRKM Rate Constant Calculations[a]

Cp_2Mn(6)	2, 53, 59, 135, 136, 186, 189, 200, 307, 596, 601, 603, 607, 748, 749, 767, 768, 768, 780, 827, 828(3), 859, 869, 874, 884, 987, 988, 990, 991, 1029, 1031, 1032, 1034, 1080, 1083, 1260, 1260, 1325, 1328, 1329, 1332, 1425(2), 1429, 1430, 3028, 3029(3), 3045(4), 3057(2)
Cp_2Mn^+(3)	18, 36, 75, 120, 165, 168, 249, 267, 330, 409, 492, 541, 574, 577, 734, 791, 801, 806, 808, 810, 814, 822, 823, 851, 873, 886, 894, 937, 949, 966, 984, 990, 1009, 1034(2), 1072, 1095, 1182, 1259, 1263, 1326, 1331, 1358, 1372, 1418, 1424, 1494, 3049(2), 3058, 3061, 3062(2), 3067, 3072, 3075, 3081
TS	−120,[b]18, 6, 8, 15, 16, 20, 267, 330, 409, 492, 541, 574, 577, 734, 791, 801, 806, 808, 810, 814, 822, 823, 851, 873, 886, 894, 937, 949, 966, 984, 990, 1009, 1034(2), 1072, 1095, 1182, 1259, 1263, 1326, 1331, 1358, 1372, 1418, 1424, 1494, 3049, 3049, 3058, 3061, 3062(2), 3067, 3072, 3075, 3081

[a] Calculated at the HF/6-31G*:LANL2DZ level and scaled by the factor 0.893;[30] the numbers in parentheses are either the spin multiplicities, or the degeneracy in the vibrational frequency. [b] Reaction coordinate.

The Cp loss reactions of the Cp_2Mn^+ ion are expected to be direct dissociation reactions without reverse activation barriers. The frequencies of the transition states for these reactions can be calculated by using variational transition state theory (VTST).[26−28] Instead of performing VTST calculations, as was done for the case of $CpCo(CO)_2$,[29] we used simple RRKM theory to model the dissociation rates and varied the transition state frequencies until theory and experimental data agreed. Because the transition state is very loose at low ion internal energies, the rate data are in the phase space limit so that the derived dissociation limits should be accurate. That is, the transition state is located at very large $CpMn^+$−Cp distances where the energy is very close to the dissociation energy. The transition state frequencies were estimated by using those of the molecular ion, Cp_2Mn^+, by deleting the 120 cm^{-1} frequency. The frequency is assigned as the Cp−Mn bond stretch vibration, which will become the reaction coordinate as the Cp_2Mn^+ ion dissociates. For each spin state, the lowest vibration was treated as a hindered internal rotation of the Cp ring, while the next five frequencies were adjusted to fit the experimental results. As the Cp_2Mn^+ ion dissociates, these six frequencies convert into the translational and rotational degrees of freedom of the products. The frequencies used in the calculations of the thermal energy distribution and RRKM rate constants are listed in Table 1.

Results and Discussion

1. The simulation of TOF Distributions and Breakdown Diagram. TOF mass spectra of Cp_2Mn were collected in the photon energy range of 10.0 → 14.0 eV. Typical TOF distributions are shown in Figure 2, in which the points are the experimental data and the solid lines the best fit to the data. The ion peak at about 31.4 μs is the molecular ion, Cp_2Mn^+ (m/z 185), whereas the TOF of the product ion, $CpMn^+$(m/z 120), is spread out between 25.0 and 29.0 μs. The asymmetry is a result of the slow dissociation. These results, similar to the electron ionization studies,[11,12] show that the primary fragmentation of Cp_2Mn^+ corresponds to the loss of a neutral fragment of mass 65, i.e., the Cp ligand, as shown in eq 1:

$$Cp_2Mn^+ \rightarrow CpMn^+ + Cp \qquad (1)$$

Figure 2 shows that the molecular ion peak is comprised of two parts: a central sharp peak (about 10%) on top of a broad peak (90%). The sharp peak results from the effusive jet produced by the sample inlet, while the broader peak results from the Cp_2Mn vapor in the background. The former corresponds to a lower translational temperature, but most likely a room temperature internal energy distribution. In the simulations (discussed later), we used two Gaussian functions with different full-width-half-maximum values to convolute with the calculated intensity distributions of the parent ion and the daughter ion. Because the sharp peak comprises only 10% of the signal, and because the slow dissociation and kinetic energy release in the dissociation broaden the fragment ion distributions, this sharp peak is not evident in the fragment ion TOF distributions.

(26) Baer, T.; Hase, W. L. *Unimolecular Reaction Dynamics: Theory and Experiments*; Oxford University Press: New York, 1996.
(27) Wardlaw, D. M.; Marcus, R. A. *Adv. Chem. Phys.* **1988**, *70*, 231−263.
(28) Hase, W. L. *Chem. Phys. Lett.* **1987**, *139*, 389−394.
(29) Sztáray, B.; Baer, T. *J. Am. Chem. Soc.* **2000**, *122*, 9219−9226.

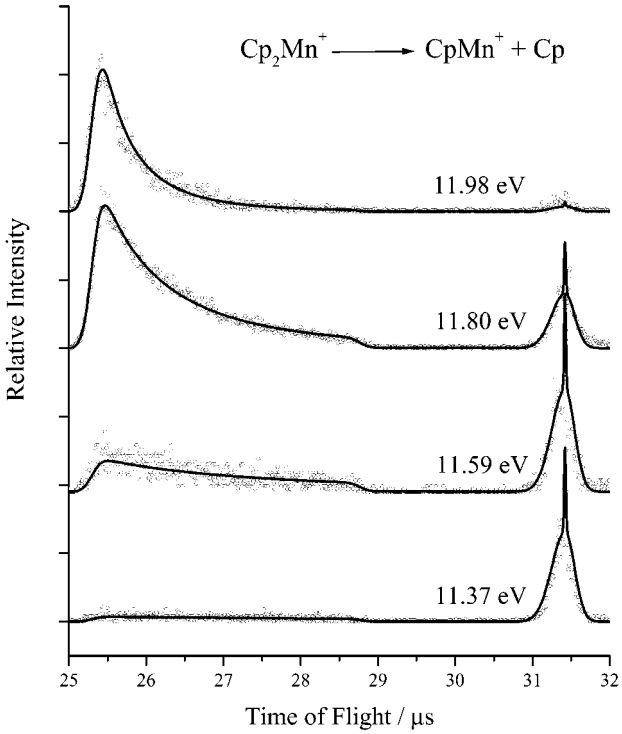

Figure 2. Ion time-of-flight distributions at different photon energies. The points are the experimental data and the solid lines are the simulation results using the RRKM rate data in Figure 4.

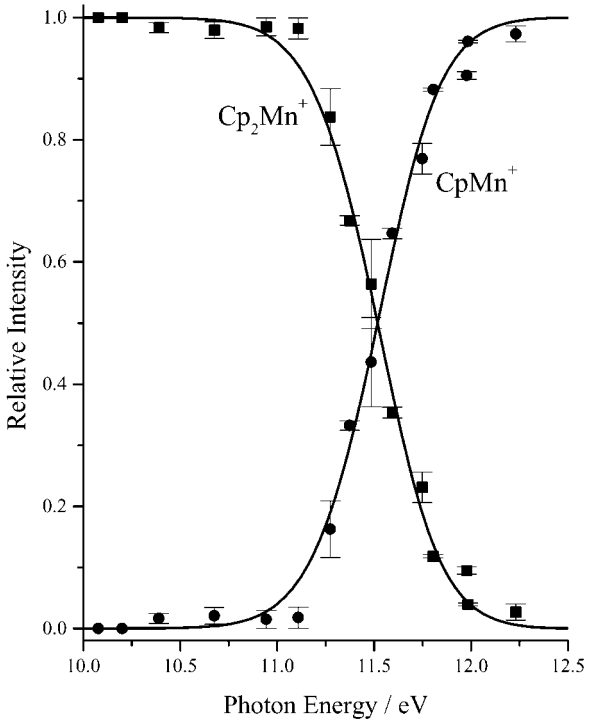

Figure 3. Breakdown diagram of the dissociation reaction of Cp_2Mn^+. The points are the experimental data with error estimates, and the solid lines are the simulation results, assuming a 0 K dissociation limit of 9.55 eV, and the RRKM rate data in Figure 4.

The TOF data in Figure 2 not only provide information about the absolute dissociation rates of the parent ion, but also provide branching ratios of parent and daughter ion signals. Figure 3 shows these branching ratios as a breakdown diagram of the Cp_2Mn^+ ion, in which the points are the experimental ratios with error estimates, and the solid lines are the simulation results. The electron ionization experiments reported Mn^+ onsets associated with the loss of two Cp units of 13.6 eV[11] and 12.57 eV.[12] However, we observed no Mn^+ ions up to a photon energy of 14.0 eV. This discrepancy will be discussed later.

As shown in Figure 2, the $CpMn^+$ ion TOF distributions are asymmetric at the energies close to the appearance energy of the $CpMn^+$ ion. This indicates that the $CpMn^+$ ion is produced while its parent ion is accelerating in the first acceleration region. The unimolecular dissociation rate constants of the Cp_2Mn^+ ion in eq 1 were calculated by using statistical RRKM theory:[26]

$$k(E) = \frac{\sigma N^{\ddagger}(E - E_0)}{h\rho(E)} \qquad (2)$$

in which E_0 is the activation energy, $N^{\ddagger}(E - E_0)$ is the sum of states of the transition state from 0 to $E - E_0$, and ρ(E) is the density of states of the ion. σ is the symmetry parameter, which is 2 for either of the two sets of spin states.

To fit the data in Figures 2 and 3, it is necessary to interpret the rate constants in terms of a thermal distribution of the Cp_2Mn^+ precursor ion. The energy distribution of the precursor ion was calculated by convoluting the electron energy analyzer function with the thermal energy distribution of the neutral Cp_2Mn molecule. The thermal energy distribution of the neutral Cp_2Mn molecule was calculated by using the Boltzmann distribution:

$$P(E) = \frac{\rho(E)e^{-E/RT}}{\int_0^{\infty} \rho(E)e^{-E/RT}\,dE} \qquad (3)$$

in which the rovibrational density of states, $\rho(E)$, is calculated by using a direct count method.[26] The Cp_2Mn molecule is approximately a symmetric top with the rotational constants (A = 2229 MHz, $B = C$ = 704 MHz for the sextet state). The analyzer function was measured from a threshold photoelectron spectrum of acetylene, which has widely spaced energy levels. However, as discussed by Li et al.,[2] some adjustments of this function are necessary in cases where the dissociation onset falls in a Franck−Condon gap region of the photoelectron spectrum.

Gas-phase electron diffraction experiments[31] suggest that cobaltocene, a similar compound, has nearly freely rotating Cp rings. Because DFT calculations[18] also indicate that the energy barrier of the Cp ring rotation is less than 2.5 kJ/mol, the lowest frequency mode of Cp_2Mn, which is assigned as the internal rotation of the Cp ring, was treated as a hindered rotation (a Pitzer rotor). Similarly, the lowest vibrational mode of the Cp_2Mn^+ ion was also assigned as the internal rotation of the Cp ring and thus was treated as a hindered rotation. The above DFT result of 2.5 kJ/mol is used as the estimated rotational barrier heights for neutral and ionic Cp_2Mn.

The ion TOF distributions and the breakdown diagram can be calculated by using the following known information: the thermal energy distribution of the Cp_2Mn^+ ion, the acceleration electric fields and the acceleration and drift field distances, and the adiabatic ionization energy of Cp_2Mn (6.12 ± 0.07 eV).

(30) Pople, J. A.; Scott, A. P.; Wong, M. W.; Radom, L. *Isr. J. Chem.* **1993**, *33*, 345−350.
(31) Hedberg, A. K.; Hedberg, L.; Hedberg, K. *J. Chem. Phys.* **1975**, *63*, 1262−1266.

The adiabatic ionization energy was calculated from the measured electron-transfer Gibbs free energy of 142.5 kcal/mol (6.18 eV).[9] Our calculated ΔS_{ioniz} based on the ground-state to ground-state transition ($^6A \rightarrow {}^3E$) is -16.7 J·K^{-1}·mol^{-1}, which at 350 K (the temperature of the electron-transfer experiment) yields a $T\Delta S$ term of -0.06 eV, from which we calculate a ΔH_{ioniz} of 6.12 eV. Because the rate constants are dominated by two variables, the dissociation energy and the activation entropy, by adjusting the dissociation energy, the vibrational frequencies of the transition state, and to a limited extent the threshold electron analyzer function, the experimental breakdown diagram and TOF distributions can be fitted simultaneously. This calculation method, which has been previously described in detail by Keister et al.[32] and Sztáray and Baer,[29] can be used to extract accurate thermochemical onsets and bond energies.

Although only the ground-state (^3E) ionic frequencies are listed in Table 1, we also used the excited-state (^1E) vibrational frequencies for the RRKM rate calculations. These analyses showed that for both the high-spin and low-spin sets of frequencies, the best fits to the experimental data were obtained with an almost identical 0 K thermochemical dissociation limit of 9.55 eV. The simulated TOF distributions and breakdown diagram are shown in Figures 2 and 3, respectively.

To estimate the uncertainty of the above dissociation onset, we fixed the dissociation energy at different values and only adjusted the frequencies of the transition state (also to a limited extent the threshold electron analyzer function) to fit the experimental results. It was found that the optimized frequencies of the transition state varied with the change of the assumed dissociation energy so that a range of dissociation limits could be accommodated. However, any variance of the dissociation energy in excess of 0.15 eV resulted in a significantly worse simulation quality. We also tested the sensitivity of the optimized dissociation energy on the assumed rotational barrier by multiplying the rotational barrier by a factor of 0.5→2. The simulation shows that the optimized dissociation limit agreed with the original one to within less than 0.01 eV. A similar insensitivity of the derived dissociation onset was noted when the assumed Cp_2Mn ionization energy was varied by ± 0.07 eV. That is, if the IE was raised, the optimized dissociation energy was lowered by a corresponding amount, resulting in a constant AE value. Thus, the error limit of the $CpMn^+$ ion appearance energy quoted in this study is ± 0.15 eV. Using this 0 K thermochemical dissociation limit, combined with the adiabatic IE value of Cp_2Mn, the $CpMn^+-Cp$ bond energy can be derived to be 3.43 ± 0.17 eV.

The RRKM calculated rate constant curve used in the best fit is shown in Figure 4. The activation entropy for this dissociation, calculated with the molecular ion and transition state vibrational frequencies, is 75.0 J·K^{-1}·mol^{-1} at 600 K. This large positive value indicates that the dissociation reaction proceeds via a very loose transition state, as expected for a simple bond-breaking reaction. A remarkable feature of the $k(E)$ curve in Figure 4 is the slow rate constant at the dissociation limit. Even at 11.37 eV (1.82 eV above the dissociation limit) the fragment peak TOF distribution in Figure 2 is extremely asymmetric. This slow rate at low energies results in a shift of the observed onset by about 1.5 eV. That is, we do not observe a $CpMn^+$ ion unless it dissociates in about 10 μs. This is also evident in Figure 3, where the fragment ion signal first appears at around 11 eV, while the derived dissociation onset is 9.55 eV. This shift is consistent with the results in Figure 4, where the rate constant of about 10^4 s^{-1} corresponds to an excess energy of about 1.7 eV. It is primarily this large kinetic shift and the resulting extrapolation of the $k(E)$ curve in Figure 4 that is responsible for the large uncertainty of ± 0.15 eV in the derived dissociation limit.

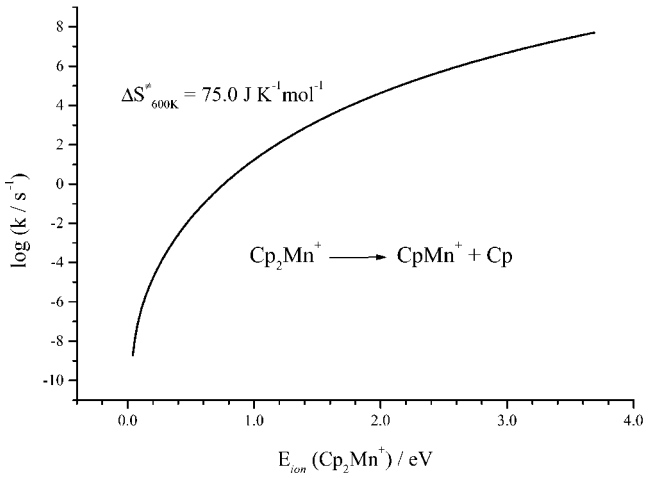

Figure 4. RRKM calculated rate curve of the Cp loss reaction determined by fitting the rate data in Figures 2 and 3.

While kinetic shifts have been observed and discussed for many years,[33−35] its magnitude in the case of the Cp_2Mn^+-dissociation ranks this example among the largest yet observed. It is a result of the strong $CpMn^+-Cp$ bond energy and the large number of vibrational frequencies in this molecule. Of course, the shift is also a function of the experimental observation time. The onset could be shifted to lower energies by storing the parent ions in a trap where they can dissociate prior to mass analysis.[36] However, as pointed out by Huang and Dunbar,[33] this works only down to a rate constant of about 10^2 s^{-1}, below which IR fluorescence stabilizes the ion before it can dissociate. In the case of Cp_2Mn^+, this limit is reached at an energy of 1 eV above its thermochemical dissociation limit. That is, no matter how long one stores the ions, they will not dissociate.

As previously mentioned, the electron ionization appearance energy of $CpMn^+$ reported by Müller and D'or[11] is 11.09 ± 0.1 eV, which agrees quite well with our own phenomenological appearance energy obtained from the breakdown diagram in Figure 3. This similarity suggests that the time for ion extraction out of the ionization region in these two experiments (ca. 10 μs) is probably similar. On the other hand, the more recent electron ionization study of Opitz[12] suggests a dissociation limit of 9.36 ± 0.3 eV. While a somewhat lower appearance energy is expected because the Opitz study detected only those $CpMn^+$ ions produced by long-lived metastable parent ions, the reported onset is not only lower than our extrapolated onset of 9.55 eV, it is 1.3 eV lower than the limit imposed by ion stabilization due to infrared emission. We can offer no reasonable explanation

(32) Keister, J. W.; Baer, T.; Thissen, R.; Alcaraz, C.; Dutuit, O.; Audier, H.; Troude, V. *J. Phys. Chem. A* **1998**, *102*, 1090−1097.
(33) Huang, F. S.; Dunbar, R. C. *J. Am. Chem. Soc.* **1990**, *112*, 8167−8169.
(34) Lifshitz, C. *Mass Spectrom. Rev.* **1982**, *1*, 309−348.
(35) Chupka, W. A. *J. Chem. Phys.* **1959**, *30*, 191−211.
(36) Lifshitz, C.; Gotchiguian, P.; Roller, R. *Chem. Phys. Lett.* **1983**, *95*, 106−108.

Table 2. Thermochemical Results (in kJ/mol)[k]

species	$\Delta_f H°_{298K}$	$\Delta_f H°_{0K}$	$H°_{298K} - H°_{0K}$
Cp_2Mn	276.9 ± 3.0[a]	299.9 ± 3.0[b]	34.88[c]
Cp_2Mn^+	863 ± 7[d]	890 ± 7[e]	30.56[f]
$CpMn^+$	935 ± 16[d]	947 ± 16[g]	19.48[f]
Cp	262 ± 4[h]	274 ± 4[h]	14.3[h]
Mn	283.3 ± 4.2[i]	282.1 ± 4.2[i]	
Mn^+	1000.789 ± 0.5[j]	999.6 ± 0.5[i]	

[a] Webbook.[38] [b] $\Delta H°_{298K} \rightarrow \Delta H°_{0K}$. [c] Rabinovich et al.[39] [d] $\Delta H°_{0K} \rightarrow \Delta H°_{298K}$. [e] $\Delta_f H°_{0K}$(neutral) + IE(Cp_2Mn). [f] Determined from the HF calculated vibrational frequencies. The spin multiplicity for $CpMn^+$ is 6.[2] [g] $\Delta_f H°_{0K}$(neutral) + AE($CpMn^+$) − $\Delta_f H°_{0K}$(Cp). [h] The heat of formation of the C_5H_5 radical has recently been remeasured[40] and compared to very high quality ab initio methods.[41,42] The two approaches agree to within the experimental error. [i] NIST-JANAF thermochemical tables.[43] [j] NIST-JANAF thermochemical tables,[43] converted to the ion convention. [k] In the $H°_{298K} - H°_{0K}$ calculations, the heat capacity of the electron was treated as 0.0 kJ/mol at all temperatures (the ion convention[37]). To convert to the electron convention, which treats the electron as a real particle, 6.197 kJ/mol should be added to the 298 K heat of formation of each ion.

for this value unless it was caused perhaps by collision-induced dissociation of vibrationally excited ions.

2. The Thermochemical Results. The 298 and 0 K thermochemical data of all relevant molecules and ions in this study are listed in Table 2.

The TPEPICO study only determines the appearance energies and bond energies. To obtain thermochemical values of Cp_2Mn^+ and $CpMn^+$, the 298 K heat of formation of neutral Cp_2Mn listed in Webbook[38] is used as the reference value. The 0 K heat of formation of neutral Cp_2Mn was calculated by using the following equation:

$$\Delta_f H°_{0K}(Cp_2Mn) = \Delta_f H°_{298K}(Cp_2Mn) - [H°_{298K} - H°_{0K}](Cp_2Mn) + [H°_{298K} - H°_{0K}](\text{elements}) \quad (4)$$

where the $[H°_{298K} - H°_{0K}]$ function was determined by using the HF calculated vibrational frequencies, and "elements" refers to the sum of the elements in their standard states. In this case, they are $10C(s) + 5H_2(g) + Mn(cr)$, whose values are C(s) 1.050 kJ/mol, H_2(g) 8.468 kJ/mol, and Mn(cr) 4.996 kJ/mol, respectively.[44]

The 0 K heat of formation of $CpMn^+$ is obtained to be 947 ± 16 kJ/mol by using the equation:

$$\Delta_f H°_{0K}(CpMn^+) = \Delta_f H°_{0K}(Cp_2Mn) + \text{AE}(CpMn^+) - \Delta_f H°_{0K}(Cp) \quad (5)$$

The 0 K heat of formation of the Cp_2Mn^+ ion is calculated by adding the adiabatic ionization energy of 6.12 eV to $\Delta_f H°_{0K}(Cp_2Mn)$, resulting in the 0 K heat of formation of 890 ± 7 kJ/mol. The 298 K heats of formation of Cp_2Mn^+ and $CpMn^+$ were calculated in a similar equation as eq 4 but now with the $[H°_{298K} - H°_{0K}]$ values for the ions.

The Mn^+ ion, which is the dissociation product of $CpMn^+$, was not observed in the experimental photon energy range up to 14 eV. Thus, we cannot directly determine the Cp−Mn^+ bond energy. However, using the known heats of formation of Cp and Mn^+ and the above-derived heat of formation of $CpMn^+$, a Cp−Mn^+ bond energy of 3.38 ± 0.20 eV can be derived. This agrees quite well with the Cp−Mn^+ bond energy of 3.10 ± 0.10 eV derived in a recent TPEPICO study of $CpMn(CO)_3$.[2] The latter study was based on a combined analysis of experimental Mn^+−CO bond energies and DFT calculations.

The thermochemical onset for the Mn^+ ion from Cp_2Mn can now be calculated to be 12.9 eV. This value is 1.1 eV lower than 14.0 eV, the maximum photon energy of our light source. Two factors explain this nonobservance of Mn^+. First, the Cp ligand carries away a great deal of internal vibrational energy in the first dissociation step, $Cp_2Mn^+ \rightarrow CpMn^+ + Cp$. We estimate on the basis of a statistical distribution of energies that at a photon energy of 14 eV, the Cp ligand carries off an average of about 2 eV of internal energy. Because of the large number of vibrational modes, the distribution of Cp internal energy will be fairly narrow. Second, as in the case of the first Cp loss process, the $CpMn^+$ ion is metastable and requires significant excess energy before the rate constant is sufficiently fast to permit seeing the final dissociation product, Mn^+. These two factors evidently shift the onset to energies above 14.0 eV. As in the case of the $CpMn^+$ onset, the electron ionization experiment of Opitz[12] finds a Mn^+ onset of 12.57 eV, which is below our calculated onset of 12.9 eV.

With use of the known heats of formation of Mn, Cp, and the Cp_2Mn molecule, the sum of the bond energies of the two Cp−Mn bonds in neutral Cp_2Mn is derived to be 5.50 eV. On the basis of scaled DFT calculation results, the Cp−Mn bond energy was reported as 2.16 ± 0.20 eV.[2] Subtracting the Cp−Mn bond energy from the sum of the two bond energies permits us to determine the neutral CpMn−Cp bond energy to be 3.34 eV. This value is some 1.18 eV higher than the Cp−Mn bond energy, a trend that is consistent with Cp_2Fe, whose CpFe−Cp bond energy is nearly 1.3 eV higher than that of the Cp−Fe bond.[9]

The 0 K ionization−dissociation energy diagram of the Cp_2Mn system can be obtained by combining the above two Cp−Mn bond energies of neutral Cp_2Mn, the IE values of Mn (7.44 eV)[43] and Cp_2Mn, and the bond energies of Cp_2Mn^+, as shown in Figure 5. The energies listed in the figure are the 0 K heats of formation or the sum of the heats of formation of the species. Because the ionization energy of Mn is higher than that of Cp_2Mn, the sum of the two Cp_2Mn bond energies in the ion is higher than the sum in the neutral Cp_2Mn. The HOMO of the Cp_2Mn molecule is the e_{1g} orbital,[45] which is an antibonding orbital. The loss of one electron from this orbital (d_{xz} and d_{yz} of Mn[18]) will thus strengthen the Cp−Mn bonds, thereby explaining the higher ionic bond energies.

The accuracy of the Cp−Mn^+ bond energy determined in this study depends on the assumed heat of formation of neutral Cp_2Mn. This value seems to be quite well established in that

(37) Rosenstock, H. M.; Draxl, K.; Steiner, B. W.; Herron, J. T. *Journal of Physical Chemistry Reference Data*; Vol. 6, Energetics of gaseous ions; American Chemical Society: Washington, DC, 1977.
(38) http://webbook.nist.gov/chemistry/om/. 2000.
(39) Rabinovich, I. B.; Nistratov, V. P.; Telnoy, V. I.; Sheiman, M. S. *Thermochemical and Thermodynamic Properties of Organometallic Compounds*; Begell House, Inc.: New York, 1999.
(40) Roy, K.; Braun-Unkhoff, M.; Frank, P.; Just, Th. *Int. J. Chem. Kinet.* **2001**, *33*, 821−833.
(41) Nguyen, T. L.; Le, T. N.; Mebel, A. M. *J. Phys. Org. Chem.* **2001**, *14*, 131−138.
(42) Kiefer, J. H.; Tranter, R. S.; Wang, H.; Wagner, A. F. *Int. J. Chem. Kinet.* **2001**, *33*, 834−845.
(43) Chase, M. W. *NIST-JANAF Thermochemical Tables*; American Institute of Physics: New York, 1998.
(44) Wagman, D. D.; Evans, W. H. E.; Parker, V. B.; Schum, R. H.; Halow, I.; Mailey, S. M.; Churney, K. L.; Nuttall, R. L. *The NBS Tables of Chemical Thermodynamic Properties*; J. Phys. Chem. Ref. Data, Vol. 11, Suppl. 2; NSRDS, U.S. Government Printing Office: Washington, DC, 1982.
(45) Famiglietti, C.; Baerends, E. J. *Chem. Phys.* **1981**, *62*, 407−421.

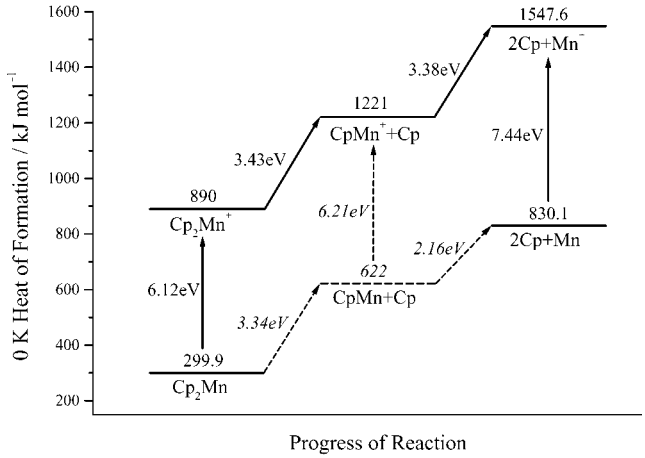

Figure 5. 0 K heat of formation diagram for the ionization and dissociation of the Cp_2Mn system. The solid lines and arrows show the experimentally determined energies, while the dashed lines and arrows are the results based on the DFT calculations. The ionization energy of CpMn is the energy difference between the ion and the neutral ground states.

the 298 K values listed in the Webbook[38] (276.9 ± 3.0 kJ/mol), the GIANT (277 kJ/mol) by Lias et al.,[46] and the recent critical compilation of Rabinovich et al.[39] (272 ± 3 kJ/mol) are very close to each other, and are based on several independent static-bomb calorimetry measurements.[47−49] This is in stark contrast to the situation encountered in our previous $CpMn(CO)_3$ study,[2] for which the Webbook values for the heat of formation of $CpMn(CO)_3$ varied over 80 kJ/mol. In that study, we suggested a better $\Delta_f H°_{0K}(CpMn(CO)_3)$ of −403 ± 15 kJ/mol, based on the combined experimental ionic $Cp(CO)_nMn^+-CO$ ($n = 0 \rightarrow 2$) bond energies and a scaled DFT calculation. However, since the publication of that paper, a new heat for formation of the cyclopentadienyl radical has been reported (see Table 2),[40] which raises the derived $CpMn(CO)_3$ heat of formation by 20 kJ/mol to −383 kJ/mol. We are now in a position to confirm this heat of formation because we have an independent determination of the $CpMn^+$ heat of formation. The 0 K enthalpy of reaction 6

$$CpMn(CO)_3 + h\nu \rightarrow CpMn^+ + 3CO + e^- \qquad (6)$$

is equal to the thermochemical dissociation limit, which has been experimentally determined to be 10.51 ± 0.06 eV.[2] Using this value and the $\Delta_f H°_{0K}(CO)$ of −113.80 kJ/mol, the $\Delta_f H°_{0K}(CpMn(CO)_3)$ is found to be −408 ± 17 kJ/mol, which is within the error limits, equal to the previously mentioned value of −383 ± 15 kJ/mol. The new 298 K value for the $CpMn(CO)_3$ heat of formation is −424 ± 17 kJ/mol.

Conclusions

The asymmetric time-of-flight distributions show that the $CpMn^+$ product ion is produced by a slow dissociation of the metastable Cp_2Mn^+ parent ion. By simulating the measured asymmetric time-of-flight peak shapes and breakdown diagram, the appearance energy for the $CpMn^+$ ion was determined to be 9.55 ± 0.15 eV. The adiabatic ionization energy of Cp_2Mn was calculated to be 6.12 eV from the reported Gibbs ionization free energy, which leads to a $CpMn^+-Cp$ bond energy of 3.43 ± 0.17 eV. By using the known heats of formation of Cp and Mn^+, the $Cp-Mn^+$ bond energy was found to be 3.38 ± 0.20 eV. The derived 298 K gas phase heats of formation of Cp_2Mn^+ and $CpMn^+$ are 863 ± 7 and 935 ± 16 kJ/mol, respectively. Combining these values with the previously determined appearance energy of $CpMn^+$ from the precursor ion, $CpMn(CO)_3^+$, leads to a $\Delta_f H°_{298K}(CpMn(CO)_3)$ of −424 ± 17 kJ/mol, thereby confirming a previous estimate of this heat of formation.

Acknowledgment. We thank the U.S. Department of Energy and the National Science Foundation through its international Programs for Eastern Europe for Financial support. B.Sz. acknowledges supports of the Hungarian Secretary of Education (Grant No. FKFP 0162/1999) and the Magyari postdoctoral fellowship. Finally, we thank the North Carolina Supercomputing Center (NCSC) for a generous allotment of computer time.

JA012682B

(46) Lias, S. G.; Bartmess, J. E.; Liebman, J. F.; Holmes, J. L.; Levin, R. D.; Mallard, W. G. *Gas-Phase Ion and Neutral Thermochemistry*; J. Phys. Chem. Ref. Data, Vol. 17, Suppl. 1; NSRDS, U.S. Government Printing Office: Washington, DC, 1988.
(47) Chipperfield, J. R.; Sneyd, J. C. R.; Webster, D. E. *J. Organomet. Chem.* **1979**, *178*, 177−189.
(48) Tel'noi, V. I.; Kir'yanov, K. V.; Ermolaev, V. I.; Rabinovich, I. B. *Dokl. Akad. Nauk SSSR* **1975**, *220*, 137−140.
(49) Pilcher, G.; Skinner, H. A. Thermochemistry of organometallic compounds. In *The Chemistry of the Metal−Carbon Bond*; Hartley, F. R., Patai, S., Eds.; John Wiley & Sons, Ltd: New York, 1982; pp 43−90.